

Large-scale production, purification and crystallization of wild-type adeno-associated virus-2

Qing Xie^{a,b,1}, Joan Hare^{a,b,2}, Joy Turnigan^{a,b}, Michael S Chapman^{a,b,*}

^a Kasha Laboratory of Molecular Biophysics, Florida State University, USA

^b Department of Chemistry and Biochemistry, Florida State University, USA

Received 13 April 2004; received in revised form 8 July 2004; accepted 19 July 2004

Available online 1 September 2004

Abstract

Adeno-associated virus-2 (AAV-2) has long been recognized as a potential vector for human gene therapy. Although much progress has been made in the molecular virology of AAV-2, structural studies of AAV-2 have been hampered by the low efficiency of virus production in culture, the low purity of preparations, and the low solubility of pure virus particles in solution. Methods of larger scale AAV-2 production have been developed through adaptation to suspension culture and re-optimization of the times of infection and transfection with respect to particle production. The methods allow the purification of 10 mg (~10¹⁵ particles) of AAV-2 per preparation at ~99% purity as judged by SDS-PAGE. This was sufficient for the screening of conditions for the formation of diffraction-grade crystals, ultimately leading to an atomic structure for AAV-2.

© 2004 Elsevier B.V. All rights reserved.

Keywords: Gene therapy; Vector

1. Introduction

Adeno-associated virus-2 (AAV-2) was identified more than a decade ago as a potential vector for human gene therapy. Because of its great promise it has been the subject of intense scientific scrutiny. Much of the basic molecular biology of the virus is now well known, including the roles of

the protein products of the two genes, *rep* associated with genome replication (Batchu and Hermonat, 1995; Chiorini et al., 1996; Davis et al., 2000; Hermonat et al., 1998; Im and Muzyczka, 1990; Li et al., 1997) and *cap* that encodes the capsid structural proteins (Vincent et al., 1997; Weger et al., 1997), in the replication and integration of the virus (Young et al., 2000). Human adeno-associated viruses belong to the *Dependovirus* genus of the parvoviruses, and are satellite viruses requiring helper functions to be provided in *trans* by a “helper” virus, most commonly adenovirus (Carter, 1990). The receptors on the cell surface used by AAV-2 to gain entry have been identified (Mizukami et al., 1996; Qiu et al., 2000; Summerford and Samulski, 1998) as have several antigenic epitopes on the virus coat surface (Moskalenko and Chen; Wobus et al., 2000; Wu et al., 2000). The attachment of single AAV-2 particles, entry into, and subsequent movements within a human cell have been mapped by single-molecule fluorescence microscopy (Seisenberger et al., 2001), and the location of site-specific integration into the human genome has been identified (Kogure et al., 2001; Linden et al., 1996).

Abbreviations: AAV-2, adeno-associated virus 2; CAPS, 3-cyclohexylamino-propanesulfonic acid; DMEM, Dulbecco's modified Eagle's medium; HEPES, *N*-(2-hydroxy) piperazine-*N'*-(2-ethanesulfonic acid); HMG buffer, HEPES/Mg⁺⁺/glycerol buffer; JMEM, Joklik minimum essential medium; LDS-PAGE, lithium dodecyl sulfate polyacrylamide gel electrophoresis; MES, 2-(*N*-morpholino)ethanesulfonic acid; PEG, polyethylene glycol; PEG MME, PEG monomethylether; rAAV-2, recombinant adeno-associated virus 2; TBS, Tris-buffered saline; VP1 (or 2 or 3), viral protein 1 (or 2 or 3); w, wild type

* Corresponding author. Tel.: +1 850 644 8354; fax: +1 850 644 7244.

E-mail addresses: qingxie@sb.fsu.edu (Q. Xie), hare@sb.fsu.edu (J. Hare), chapman@sb.fsu.edu (M.S. Chapman).

¹ Tel.: +1 850 644 1626; fax: +1 850 644 7244.

² Tel.: +1 850 644 1640; fax: +1 850 644 7244.

Building from this knowledge, many recombinant AAV constructs (rAAV) have been developed in which AAV's genes have been replaced by potentially therapeutic genes (Bueler, 1999; Hermonat et al., 1997), mostly using serotype 2.

Our recent report of the structure of AAV-2 at atomic resolution (Xie et al., 2002) provided a further basis for rational modification of rAAV-2 in vector development (Rabinowitz and Samulski, 2002). There is strong interest in developing AAV-2 capsids with altered antigenicity to facilitate repeated gene therapy treatments of individuals that are seropositive through prior natural or therapeutic exposure. There is also interest in retargeting rAAV to different tissues through ablation of normal receptor interactions, and insertion of new ligand-binding motifs (Girod et al., 2002; Grifman et al., 2001; Ried et al., 2002; Wendtner et al., 2002). The structure of AAV-2 has allowed prior genetic and mutagenic studies of receptor-binding and antigenicity (Girod et al., 1999; Moskalenko and Chen, 2000; Summerford and Samulski, 1998; Wobus et al., 2000; Wu et al., 2000) to be integrated into a coherent picture, and now allows modifications to be designed rationally. Progress towards the atomic structure of AAV-2 by several groups was, for a long time, limited by the availability of large quantities of pure virus which was also notoriously insoluble at high concentration in the buffers usually used for crystallization. Here are reported the methods used to overcome these limits in the recent structural work. They will be useful in structural characterization of modified capsids during iterative re-engineering, and to prepare virus for other biophysical characterizations.

About 10 mg of 99% pure wild-type AAV-2 can be produced using extensions, reported here, of the classic methods of Winocour et al. (1992). It is a two-step process in which the first viral propagation in HeLa cells is initiated by both transfection with an AAV-2 infectious plasmid clone (Laughlin et al., 1983) and co-infection with helper adenovirus. The crude lysate from this first step, is then used to inoculate a secondary infection. Infectivity and normal replication had previously been the prime considerations in development of these methods, but in this work, it was particle production that was maximized. Ten to 20-fold improvements in efficiency were attained through adaptation of the cell culture to roller bottles or suspension. Conditions were also established that permitted the concentration of virus to >16 mg/ml at neutral pH, a prerequisite for the screening for crystallization conditions which ultimately led to the atomic structure.

Our work has focused on wild-type AAV-2 (wtAAV-2), not any of the rAAV constructs being developed for gene therapy. The capsid-host interactions of receptor attachment and antibody recognition that were of interest are the same in wild-type-like and current rAAV constructs. Wild-type structure was more tractable, because of the greater difficulties of producing rAAVs in large quantity (Potter et al., 2002; Urabe et al., 2002). Additional challenges in rAAV production include provision of the functions of genes replaced in the construct, minimizing wild-type reversion, and the restriction to clinically compatible purification methods in separating rAAV

from potentially pathogenic helper virus. These challenges are being met with a variety of approaches including additional plasmids or modified cell lines providing the helper or missing AAV functions (for example: Bueler, 1999; Cao et al., 2000; Clark et al., 1995; Drittanti et al., 2000; Grimm et al., 1998; Grimm and Kleinschmidt, 1999; Inoue and Russell, 1998; Matsushita et al., 1998; Ogasawara et al., 1999; Urabe et al., 2000). The current work with wt-AAV will benefit rAAV production in two ways. Firstly, it provides the quantities of virus needed to test a variety of large-scale purification methods, the best of which can then be applied to more precious rAAV preparations (Potter et al., 2002; Urabe et al., 2002). Secondly, this work will benefit attempts to re-engineer rAAV for re-targeting to different cell types or to evade immune neutralization (Bartlett et al., 1999; Buning et al., 2003; Girod et al., 1999; Huttner et al., 2003; Ried et al., 2002). The required characterization of site-directed mutants has sometimes been stymied by the difficulties of producing rAAV mutants in sufficient quantity (Huttner et al., 2003), a challenge that can be circumvented in many cases by mutating first the wild-type and taking advantage of the methods developed here.

2. Materials and methods

2.1. Plasmid and virus stocks

The plasmid pAV2 (Laughlin et al., 1983) was obtained from the laboratory of Ken Berns. It contains the complete sequence of AAV2 cloned into the plasmid pBR322. Before use in transfection, pAV2 was linearized by digestion with Bgl II. Adenovirus 2 was a gift from Erik Falck-Pedersen, Weill Medical College, Cornell University.

2.2. Cells

HeLa cells were obtained from the American type culture collection and were grown in Dulbecco's modified Eagles's medium (DMEM, Jokoby and Pastan, 1979) (Sigma) with 5% fetal calf serum (Summit Labs) and 5% newborn calf serum (Sigma) or 10% cosmic calf serum (HyClone). Monolayer cultures were grown on flasks and roller bottles (Corning). Roller bottles were initiated at 0.5 rpm and maintained at 0.75 rpm. Suspension cultures were grown in Joklik minimum essential medium (JMEM, Sigma, Cat #M0518) with 10% cosmic calf serum in Cytostir spinner flasks (Kontes) at 35–65 rpm. Cultures were incubated at 37 °C with a 5% CO₂ environment.

2.3. Production of the primary AAV/adenovirus viral stock

Approximately 3.6×10^8 cells growing in six 225 cm² flasks were transfected with 10 µg of linearized pAV2. Briefly, medium was removed from the cultures and reserved.

Cultures were rinsed twice with TBS + Ca/Mg (1.5 mM CaCl₂, 0.8 mM MgSO₄). DNA (10 μg) was added to 30 ml of freshly prepared transfection buffer (480 μg/ml DEAE-dextran in TBS + Ca/Mg). 5 ml of this transfection mixture was added to each flask which was then incubated under CO₂ for 1–2 h. Then the transfection mixture was removed and the reserved medium was restored. Four hours later, medium was replaced with DMEM/2% newborn calf serum and ~6.3 × 10⁵ pfu of adenovirus 2 stock was added to each T225 flask, containing 1.0–1.5 × 10⁸ cells at ~80% confluence. Cells and culture medium were harvested after 48 h, and subjected to three cycles of freeze/thawing.

2.4. Secondary infection for AAV production

Six roller bottles at 80–90% confluence (~1 × 10⁸ cells each; 6 × 10⁸ total) or 1–2 l of suspension culture at 0.6 × 10⁶ cells/ml (6–12 × 10⁸ total) were infected with the primary culture, containing AAV-2 and Ad-2. Medium was reduced to 0.1 volume and 1 ml of primary inoculum was added per 10⁸ cells. Cultures were incubated for 1–2 h without stirring (suspension cultures) or at slow rotation (0.25 rpm for roller bottles). The medium was replaced (now with 2% serum) and incubation at 37 °C, 5% CO₂ was continued for 40–60 h, until monitoring for cytopathic effect showed <40% viability.

2.5. Harvest and purification of virus

At ~40%, the entire culture (cells, debris and medium) was centrifuged in batches at 113,000 g in a SW28 rotor (Beckman Inc.) at 25,000 rpm for 180 min or a KA40.100 rotor (Composite Inc.) at 39,000 rpm (197,000 g) for 80 min. Pelleted virus and cell debris were resuspended in 10 ml buffer TD (140 mM NaCl, 5 mM KCl, 0.7 mM K₂HPO₄, 25 mM Tris-HCl, pH 7.4) per 3 × 10⁸ cells and lysed with the addition of trypsin (0.0125% final concentration) and sodium deoxycholate (0.5% final concentration) for 30 min at 37 °C, then homogenized with 20 strokes in a Dounce homogenizer. Cesium chloride was added to the lysate to a final concentration of 3.3 M (refractive index of 1.372) and samples were centrifuged at 38,000 rpm in a SW55 rotor (Beckman; 175,000 g), 20 °C, for 20–24 h or a Beckman 70.1Ti rotor at 51,000 rpm (239,000 g), 20 °C, for 13–16 h. The visible AAV band (Fig. 1) was collected from the middle of the tube and it was verified that the refractive index was 1.372, expected for the cesium chloride concentration corresponding to AAV's density. AAV bands from multiple tubes were pooled and the cesium gradient ultracentrifugation was repeated two more times.

2.6. Quantization of AAV yield

An aliquot from the bands recovered from the third gradient was diluted 100-fold and optical density was determined at 260 and 280 nm. A calculated extinction coefficient for empty capsids was based on the proportion of tryptophan

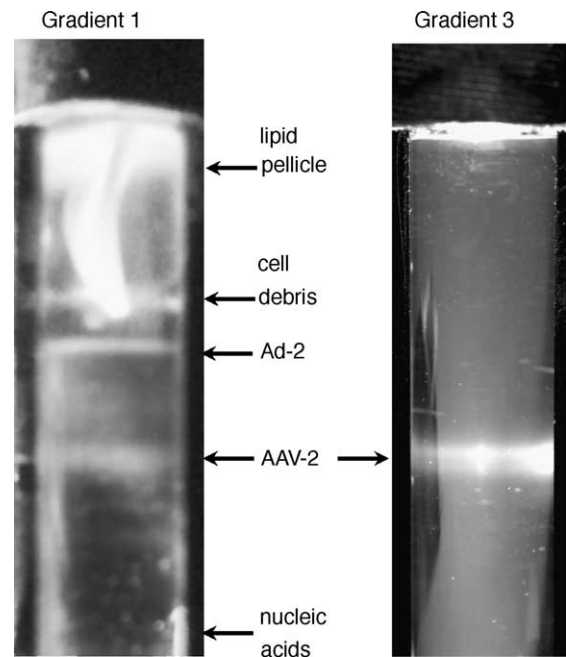


Fig. 1. Cesium gradient ultracentrifugation purification of AAV-2. After three gradients, the bands for adenovirus-2 (Ad-2) and cellular debris have disappeared. The band of adeno-associated virus-2 (AAV-2) gets stronger with pooling of the fractions from multiple tubes into a single tube for the next gradient.

and tyrosine residues in VP3, and a capsid mass that accounted for the 7.5% content of capsid protein variants VP1 and VP2. The calculated extinction coefficient for full particles used a double-stranded DNA extinction coefficient to account for the hypochromism of bases likely be predominantly stacked (Chapman and Rossmann, 1995; Freifelder, 1982). The estimated values ($\epsilon_{280} = 4.54$, $\epsilon_{260} = 7.03$ ml/(cm mg)) were not fully consistent with the empirically-determined OD₂₈₀/OD₂₆₀ ratio of 0.72 (de la Maza and Carter, 1980) that is often used to assess purity. The calculated estimates are only as good as the underlying assumptions above, and were reconciled with the empirical OD ratio, by adjusting ϵ_{260} , the estimate most dependent on the state of the DNA. Thus, for UV measurements of concentration, extinction coefficients of $\epsilon_{280} = 4.54$ and $\epsilon_{260} = 6.35$ ml/(cm mg) gave consistent results for pure virus. Both extinction coefficients are larger than had been used previously, giving lower estimated concentrations of AAV. However, they are similar to the values of 3.72 and 6.61 measured recently for denatured virus (Sommer et al., 2003) and are therefore consistent with other assay methods such as ELISA and Q-PCR. The OD₂₈₀/OD₂₆₀ ratio was used to distinguish full from empty particles, and to monitor purity. Wavelength scans were used to monitor for Rayleigh scattering.

2.7. LDS-PAGE

Samples were denatured by heating to 70° in 2% Nu-Page LDS (Invitrogen) for 10 min. Denaturing acrylamide

gels (4–12% NuPage Bis–Tris gradient) were loaded with 1 to 3 μg AAV per lane or overloaded with 10 μg to detect non-capsid or contaminant proteins. Gels were stained with Coomassie blue R-250 or G-250 (Sigma, EZ Blue) or silver nitrate.

2.8. Negative stain electron microscopy

A small quantity of AAV (10 μl at ~ 0.05 mg/ml) was loaded onto a carbon-coated 600 mesh copper hexagonal thin-line grid. One minute later, excess solution was wicked from the other side of the grid with filter paper. The sample was prepared by adding 10 μl of 2% uranyl acetate, with excess wicked away, as before, after 1 min. Samples were air-dried for 2–3 h, examined and photographed on a JEOL 1200EX transmission electron microscope operated at 100 KV.

2.9. Concentration and desalting of AAV for crystallization

Attempts were made to transfer AAV from the third Cs-gradient to various buffers, none of which was entirely satisfactory until we discovered that glycerol was a co-solvent that maintained solubility (see Section 3). In the final protocol, AAV-2 was dialyzed against HMG buffer (100 mM Hepes, 50 mM MgCl_2 , 25% glycerol and 0.03% sodium azide, pH 7.3) using a custom-built 50 μl microdialysis cell. Virus could be concentrated to approximately 16.0 mg/ml during this exchange. Once in HMG buffer, virus could also be concentrated in centrifugal Amico/Centricon-30 concentrator to approximately 9 mg/ml. Aggregates were removed by centrifugation at 16,000 g for 10 min. Concentration was determined spectrophotometrically (see above) from a 2 μl aliquot immediately before crystallization.

2.10. Microbatch crystallization

Initial screens were by the microbatch method under mineral oil (Sigma) (Chayen et al., 1992), using a 96-well plate format. AAV-2 stocks were prepared in either 100 mM acetate buffer (pH 4.5) or 100 mM HEPES (pH 7.4) with 20–50 mM Mg^{++} , and with or without 5% glycerol co-solvent. Aliquots of AAV-2 were mixed under the oil with concentrated PEG solutions (usually PEG 6000) and buffer to yield 2 μl drops containing 1.5–6.1 mg/ml AAV-2 and 1.5–4.6% PEG.

2.11. Hanging drop batch crystallization

The hanging-drop format (Hampel et al., 1968) was used for ready visualization, but, in contrast to the more usual vapor diffusion method, drop and reservoir were set up in vapor pressure equilibrium, so that there would be no change in drop concentration with time. As with the microbatch method, results are obtained within a few days, so it is suitable for rapid (crude) screening. Over 700 set-ups tested different combi-

nations of AAV-2 concentration (1.5–6.0 mg/ml) and crystallizing agent (1–5% PEG 6000) (mixed drop concentrations). Trials were all performed in 100 mM HEPES (pH 7.3) with 50 mM Mg^{++} and with or without 25% glycerol. The results were compiled into *pseudo* phase diagram (Fig. 2) to better define what started as a narrow window of productive conditions. Determination of a real phase diagram (Ducruix and Giegé, 1999; Ducruix and Ries-Krautt, 1990) requires a large number of existing crystals to determine conditions for growth and dissolution. This can be done in retrospect, but not during a search for conditions that produce the first crystals. Here, an approximate *pseudo* phase diagram was obtained by segregating the conditions in which solutions repeatedly crystallized, precipitated or nearly always remained soluble. The approximate phase boundaries that emerged were used to narrow the range of conditions to be tested for the optimal growth of large single crystals below.

2.12. Vapor diffusion crystallization

Optimization and preparation of diffraction grade crystals was by hanging-drop vapor diffusion (Hampel et al., 1968). The concentration of AAV-2 and crystallizing agent slowly increase as the drop equilibrates by vapor diffusion with a reservoir containing dehydrating agent. One hopes to pass through conditions under which (only) a few nuclei will form and then to higher concentrations needed for growth. The application here was complicated a little, because of co-crystallization with a solubilization/*cryo*-protection agent (glycerol) that, like PEG, is also a dehydrating agent. AAV-2 at ~ 8.5 mg/ml was prepared in HMG buffer (pH 7.3). Reservoir solutions contained 4–6% PEG and 25% glycerol in HMG buffer. Drops contained 2–6 μl of AAV solution mixed with an equal volume of a third solution that was identical to the reservoir except without glycerol. Thus, starting concentrations were AAV at ~ 4.25 mg/ml and PEG 6000 at 2–3%. Equilibration with the reservoir, yielded final concentrations approaching ~ 8.5 mg/ml virus and 4–6% PEG.

Vapor diffusion was also used to explore the effects of 12 common additives (McPherson, 1990), representing ions of various charges, detergents, co-solvents and mild chaotropic agents. It was also used to test for improved crystals at different temperatures and pH and with different polyethylene glycol crystallizing agents: PEG 400 (10–50%), 1000 (5–20%), 5000MME (1–10%) and 12,000 (1–3%). Together with the batch-mode screens, over 800 combinations of conditions were tested with details to be given in the results.

3. Results

3.1. Virus yields

Equivalent yields (overall and per cell) were obtained with three types of culture for the secondary infection: monolayer

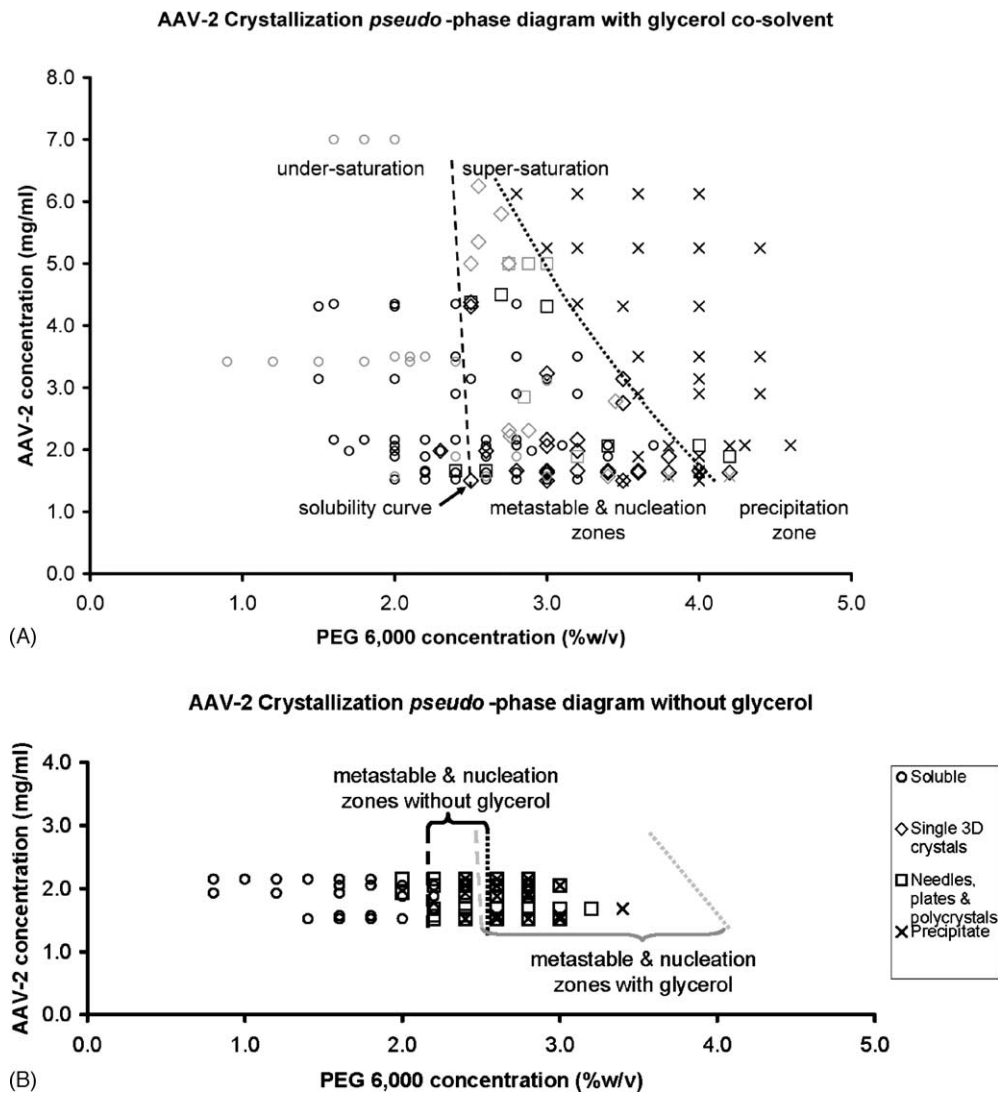


Fig. 2. *Pseudo* phase diagram for AAV-2 (A) in the presence of 25% glycerol co-solvent, and (B) without glycerol. This analysis differentiates the virus and dehydration agent concentrations most likely to lead to crystallization. Most of the data points (black symbols in A, all data points in B) were obtained by the batch method in which the concentrations of virus and PEG do not change with time. Some data points, especially at high virus concentration, were obtained with the hanging drop vapor diffusion method in which the concentrations equilibrate with time (grey data points). The values plotted were estimated for the time at which crystals or precipitate first appeared based on measured vapor diffusion rates. Measurements were made through refractive index according to the protocol of Luft and Titta (1996), using 25% glycerol solutions. Circles indicate soluble virus, crosses indicate precipitates, squares indicate needle, plate or poly-crystals, and diamonds indicate three-dimensional single crystals. The *pseudo* phase boundaries are estimated with the understanding that poorly controlled effects, such as the presence of heterologous crystallization nuclei, affect the outcome of individual crystallization attempts, rendering the data inherently noisy. For clarity, only a representative selection of the many attempts yielding soluble or precipitated virus are shown. Comparison of panels A and B shows that the effects of the glycerol are to improve the solubility and to widen the metastable/nucleation zones. The difficulty without glycerol was in finding conditions where crystals could be obtained without precipitation.

culture using 30 100 mm plates, monolayer culture using three 850 cm² roller bottles or 500 ml suspension culture. Suspension culture was the least labor-intensive and amenable to scale-up resulting in yields of ~ 10 mg (1.1×10^{15} particles) of purified virus from 3 dm³ cultures. Although the yields were high, there was significant variability, with preparations averaging $3 \pm 2 \times 10^{14}$ particles/dm³ suspension culture (or $\sim 4 \times 10^5$ particles purified from each cell).

3.2. Purity of preparations

Electron microscopy showed that, in contrast to the product of a single cesium gradient, sample from the third gradient was free of contaminating adenovirus particles (Fig. 3). Purity of virus preparations was also assessed by determining whether the OD₂₈₀/OD₂₆₀ ratio was consistent with the value of 0.72 measured for pure AAV (de la Maza and Carter, 1980), and their expected DNA/protein ratio. Following the second

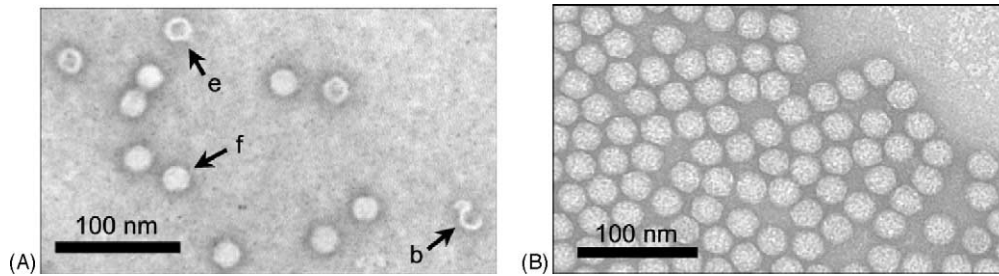


Fig. 3. Progressive purification of AAV-2 on repeated cesium gradient ultracentrifugation. Both panels are negatively stained electron micrographs photographed at 100 kV with a magnification of 80,000. Panel A shows partial purification following two gradients. Most of the particles are full (f) (DNA-containing), but there are contaminating empty (e) particles with characteristic staining of the interior, and broken (b) particles. Panel B shows a homogenous preparation of full particles following a third gradient.

cesium gradient the OD ratio was typically 0.70. Following the third ultra-centrifugation, the ratio was usually 0.72 ± 0.005 , indicating little by way of contaminating protein or nucleic acid.

Purity was also assessed through SDS-PAGE. Neither silver nor Coomassie G-250 staining revealed any contaminants in lanes loaded with 1–3 μg . As staining could detect as little as 50 ng, this demonstrated that no contaminant exceeded 5% of the AAV. A more sensitive quantitative assay was developed using serially overloaded lanes (1–10 μg) and the known ratios of VP1, 2 and 3 (1:1:8) (Johnson, 1984; Rose et al., 1971) as internal standards. The integrated density of a weak band in a heavily overloaded lane could be compared to a similarly dense band of a major capsid protein in a lane with less sample loaded. Overloaded lanes with denatured virus showed additional bands at 116, 42, 28 and 15 kDa at densities corresponding to 1–3 copies per capsid. Wistuba et al. (1995) had seen similarly size proteins in sucrose-gradient purified full and empty capsids, except that the smallest had apparent molecular weight of 10 kDa. Western analysis with the A69 monoclonal antibody had demonstrated that all were capsid protein derivatives. Western analysis of our samples (not shown) using the B1 monoclonal antibody (Wistuba et al., 1995) similarly demonstrated that these bands were all capsid protein derivatives, and that our 15 kDa band likely corresponded to the 10 kDa band of Wistuba et al. (1995). Comparison of SDS gel lanes loaded with denatured or native AAV-2 revealed that the additional bands occur only in denatured samples (Fig. 4), implying that the proteins are internal or firmly bound to the exterior of the capsid. The size of the smallest fragment corresponds approximately to the VP1 unique region, but this is likely coincidence. Wistuba et al. (1995) noted that their low molecular mass fragment increased with time post infection, as the proportion of VP3 also increased, but the implication of antibody cross-reactivity is that they share an epitope, and could not be the mutually exclusive VP3 and VP1-unique regions. Thus, the exact nature of the weak bands remains uncertain, but they are likely capsid protein degradatory products that remain sequestered with the viral assembly. The faintest band of the capsid-sequestered proteins corresponded to about 1.3% of the total protein. Proteins would be detectable at $\sim 1/10$ th of

this level, indicating that no single non-viral protein contaminant exceeds 0.1%, and that the sample is likely >99% pure.

3.3. Avoiding aggregation

At the low concentrations usually used for virological studies, AAV is soluble in physiological-like buffers. Even at 1/10th-mg/ml concentrations, it was long recognized that molar salt concentrations were needed to maintain solubility.

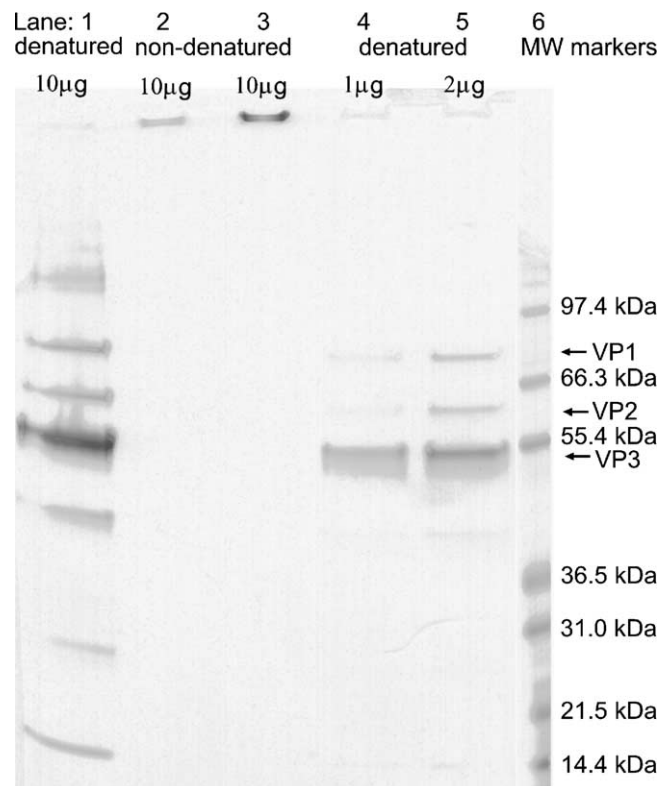


Fig. 4. LDS 4–12% acrylamide Bis–Tris gel electrophoresis of purified AAV. AAV was overloaded, at 10 μg per lane, in the first three lanes to detect minor contaminants. Lanes 4 and 5 are loaded at 1 and 2 μg , respectively. All samples except those of lanes 2 and 3 were heated (10 min, 70 °C) in denaturing buffer (2% LDS) prior to loading. The samples in lane 2 and 3 were loaded in non-denaturing and denaturing buffers respectively, but neither was heated.

High concentrations of AAV-2 in the ~ 3.3 M CsCl from ultracentrifugal purification remained mostly in solution at 4 °C, although there was some precipitation and adhesion to glass- and plastic-ware with time, even after siliconization. Buffer exchange into even 0.25 M NaCl resulted in significant loss. Lower salt buffers supporting AAV-2 concentrations of 10 mg/ml would be needed to survey possible crystallization conditions.

A large number of modifications to the buffer were tested for solubility, measuring AAV-2 recovery through OD₂₈₀, and monitoring for aggregates through the impact of Rayleigh scattering on a wavelength scan of optical density. Small samples at ~ 0.1 mg/ml AAV were used for preliminary characterization. A neutral detergent (β -octyl glucopyranoside) at sub-micellar concentrations (0.01–0.5%) led to a modest reduction in aggregation (up to 15%) that could be further improved by lowering the pH. Various buffers were tested at 25 mM in combination with 0.5% detergent: CAPS (pH 10.0), HEPES (pH 7.5), MES (pH 5.7) and acetate (pH 4.5). There was a monotonic improvement in solubility with lowering of pH, with AAV-2 appearing fully soluble at pH 4.5, but not 5.7. Several polyvalent ions were tested: a divalent cation (Mg^{++} , 20 mM) improved the solubility of samples between pH 4.5 and 7.5, whereas a trivalent anion (citrate) did not. With Mg^{++} and detergent at pH 4.5, 1–2 mg/ml was attainable at low ionic strength, enabling the start of crystallization trials. Higher virus concentrations would facilitate crystallization, so further tests of buffers continued with two co-solvents: isopropanol at 5 or 10% did not improve solubility, but 5% glycerol (25% later) greatly increased the solubility to ~ 17 mg/ml, even at pH 7.5. Excepting the glycerol, these were near-physiological conditions and became the main focus of crystallization attempts.

Although conditions were now available for maintaining solubility, concentrating the virus to high mg/ml levels efficiently still remained a challenge. Only about 20% was recovered from centrifugal concentration with an Amicon microconcentrator-100 at pH 7.5 with 5% glycerol or at pH 4.5 without glycerol. Treatment with 1% SDS showed that most of the AAV-2 had adhered to the membrane, and there was also unacceptable aggregation in the retentate. Some concentration was possible by dialysis against 5–20% solutions of PEG 12–20,000, but losses due to membrane adhesion were still high ($\sim 30\%$). The method that became our standard was found serendipitously. Higher concentrations of glycerol (25%) were being tested for co-crystallization with a cryo-protectant for subsequent freezing of crystals (Rodgers, 1994). Exchange of buffer using a microdialysis cell and a membrane with a 12–14 kDa molecular mass cutoff also resulted in increased concentration without aggregation. AAV concentration was routinely increased from ~ 4 to ~ 9 mg/ml, occasionally to 16 mg/ml, by, presumably a non-equilibrium transient process. (This corresponds to concentrations of 4.4 to 18×10^{14} particles/ml.) Higher concentrations of glycerol (25%) were later found to support the recovery of PEG-precipitated AAV-2 at up to 3.5 mg/ml, and to reduce greatly

the losses during centrifugal concentration, but these findings came after the bulk of samples for structural work had already been prepared.

High glycerol co-solvent concentrations were key to attaining high concentrations of AAV at low ionic strength. Glycerol does not appear to affect the structure greatly. Negatively stained electron micrographs at 0 and 80% glycerol appear identical. Later, isomorphous crystals would be obtained with or without the glycerol co-solvent.

The first crystals were obtained by the microbatch method (Chayen et al., 1992). Microcrystals were obtained in about 5 days with AAV-2 at 1.5–2.0 mg/ml with 2.5–3.0% PEG 6000 as crystallizing agent. Drops could be buffered at either pH 4.5 or pH 7.4, with 20–50 mM Mg^{2+} and with or without 5% glycerol co-solvent. Morphologies were plate or diamond shaped, independent of the pH. Subsequent vapor diffusion experiments explored common additives (McPherson, 1990) – salts, detergents, co-solvents, etc., and also different types of PEG. The only change leading to improvement of crystals was the addition of 25% glycerol.

To better define the narrow windows of PEG and virus concentrations conducive to crystallization, a *pseudo*-phase diagram was constructed from the results of ~ 700 batch-mode hanging-drop attempts. The concentrations in mixed drops were varied from 1.5 to 6 mg/ml in AAV-2 and 1–6% in PEG 6000. Most trials remained clear. Those where precipitate or crystalline material were often observed fell into regions similar to the precipitation and nucleation zones respectively of a theoretical phase diagram (Ducruix and Giegé, 1999; Ducruix and Ries-Krautt, 1990), which provided the basis for estimating approximate phase boundaries. Without glycerol, the metastable and nucleation zones were narrow. With glycerol, these regions were wider, making it easier to find conditions for nucleation and slow growth without precipitation (Fig. 2).

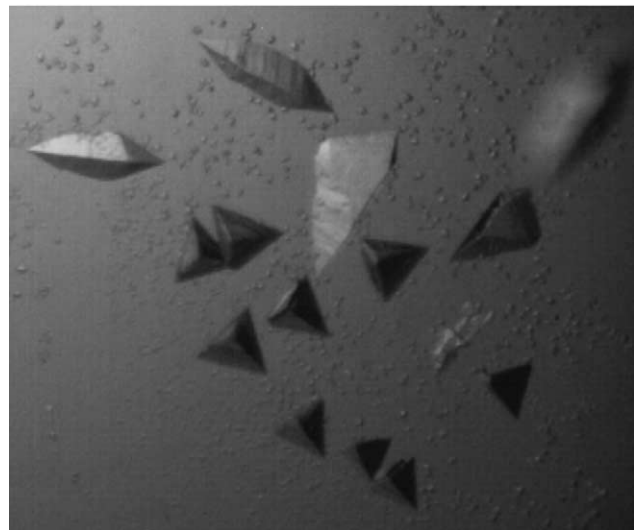


Fig. 5. Typical crystals of AAV-2. The largest usually seen have dimensions of ~ 0.3 μ m.

Larger, diffraction-grade crystals were grown by the standard hanging-drop vapor diffusion method (McPherson, 1998) for which the drop was set up at half the concentration of dehydration agent as the reservoir. After mixing the AAV-2 stock (in HMG buffer) with dehydration agent in equal 2–6 μ l volumes, the drops started at \sim 4.25 mg/ml AAV-2, 100 mM HEPES pH 7.3, 50 mM MgCl₂, 12.5% glycerol and 2.5–3.0% PEG 6000. It was equilibrated against an excess volume of 5–6% PEG in HMG buffer (i.e. 25% glycerol). Thus, vapor diffusion was driven by a two-fold difference in both PEG and glycerol concentrations, so that at equilibrium the virus concentration would approach \sim 8.5 mg/ml. Typically crystals grew to about 0.3 mm \times 0.3 mm \times 0.3 mm in a week (Fig. 5).

4. Discussion

4.1. Scalability of virus production

The prior methods were small-scale, using thirty 100 mm tissue culture plates for the secondary infection. Although the methods worked well, 10-fold + scale-up needed for crystallization trials was impractical as it has also proved for rAAV large-scale production (Urabe et al., 2002). Three roller bottles provided the same attachment surface as 30 dishes, supporting an equal number of cells and yielding the same amounts of virus. Two-fold scalability was achieved by doubling the number of roller bottles, and greater scaling could likely have been achieved if the method had not been set aside due to the time needed to establish the monolayer cultures which was several days longer.

The 3×10^8 cells, of 30 dishes or three roller bottles, could be grown in a single 500 ml suspension culture with considerably less labor. Virus yields from suspension culture, per cell, equaled or exceeded monolayer culture. Yield could be two-fold scaled by doubling the cell density at infection, and further scaled by increasing the culture volumes from 0.5 to 3 dm³. About 10 mg of virus could be produced from 31 cultures. No differences in crystallization were seen as the scale of production was increased.

4.2. Sample purity

Sample purity is usually of prime importance in protein crystallization (McPherson, 1998). Crystallization would require homogeneity of the protein capsid, whereas integrity of infectious DNA had been the prime concern in the earlier development of these methods (Winocour et al., 1992). In macromolecular purification, one usually seeks separations based on different properties, so it seemed likely that purity might be improved by substituting other methods for the second or third cesium gradient ultracentrifugation. Following methods developed for bacteriophage purification (Walsh et al., 1994), preliminary DEAE anion exchange chromatog-

raphy using a MemSep[®] cartridge (Amicon Inc.) achieved some separation, but with an unacceptably low 34% recovery. At the high concentrations needed for structural studies, the low ionic strength running buffers needed for ion exchange chromatography result in aggregation and adhesion to the apparatus. The same challenge would be faced with concentrate samples when applying the heparin affinity and ion exchange chromatographies developed more recently for rAAV (Anderson et al., 2000; Auricchio et al., 2001; Clark et al., 1999; Kaludov et al., 2002; O'Riordan et al., 2000; Summerford and Samulski, 1999; Tamayose et al., 1996; Zolotukhin et al., 1999). Our efforts with chromatography preceded our discovery of glycerol as a co-solvent, and it is possible that now conditions could be found where one of the chromatographies could be used with concentrate samples.

Having obtained crystals from cesium-gradient purified AAV-2, there was less motivation to explore these emerging chromatographic methods. In fact, SDS-PAGE indicated purity likely >99%, better than anticipated. It is likely that the high purity resulted from the large scale of our preparations, allowing us to see clearly the bands following ultracentrifugation, and to be highly selective in retaining the central fraction, discarding any tails.

4.3. The multiple effects of glycerol

With the well-known limited solubility of AAV-2, glycerol was key to obtaining concentrated solutions of AAV at low ionic strength that would be suitable for crystallization. By crystallizing in high glycerol, data collection at *cryo*-temperatures was facilitated. At 4 °C, crystals survived only \sim 1 min in a synchrotron X-ray beam, so hundreds of crystals would have been required for a complete diffraction data set. At 100 K *cryo*-protected crystals lasted up to 3 h, so that although data were collected from a few dozen crystals, only the best two were ultimately required. *Cryo*-protection is required to avoid ice crystallizing within and disrupting protein crystals, and is normally accomplished by soaking pre-grown crystals in a series of PEG, glycerol or sugar solutions chosen to avoid disordering the crystal lattice (Rodgers, 1994). Finding suitable conditions has proved more challenging for virus crystals than protein crystals for which *cryo*-methods are now used almost exclusively. By finding conditions in which AAV-2 could be crystallized in the presence of a *cryo*-protectant, this challenge was avoided. Glycerol had three effects upon crystallization. It increased the solubility of AAV-2, it broadened the nucleation zone, making it easier to obtain conditions in which just a few nuclei would grow into large crystals, and it also changed the rate of equilibration. Hanging drops of 20 μ l 12.5% glycerol equilibrated by vapor diffusion with a 25% glycerol reservoir in 11 days (as measured by refractive index), compared to 2 months for a drop of 3% PEG 6000 (alone) equilibrated against 6% PEG 6000. With the increased rate of equilibration, a colligative property, it was possible to

nearly double the virus concentration during the time-span of crystallization, driving larger crystal growth. Identical electron micrographs and crystal lattices indicate that glycerol does not have a large impact upon capsid protein conformation.

4.4. Form of the virus crystallized

The AAV capsid is comprised of proteins VP1, VP2 and VP3 in the ratio 1:1:8–10 (Johnson, 1984; Rose et al., 1971). These proteins share a common 533 residues carboxy-terminus, differing in N-terminal extensions of 65 for VP2 and another 137 for VP1, due to differential mRNA splicing. The VP1 N-terminal extension encodes for nuclear localization, phospholipase A activity and is essential for full infectivity, but not capsid formation (Girod et al., 2002; Hermonat et al., 1984; Hoque et al., 1999; Wu et al., 2000). As in prior parvovirus structures (Agbandje et al., 1993; Agbandje-McKenna et al., 1998; Simpson et al., 1998; Simpson et al., 2002; Tsao et al., 1991), the AAV-2 structure revealed only the core subunit structure common to all of the capsid proteins (Xie et al., 2002). This raised the possibility (for all the parvovirus structures) that what had been selected in crystal growth were particles lacking VP1 and/or VP2, present naturally in a heterogeneous population, or produced by artifactual proteolysis during the long time-scales of virus production and crystallization. Here, for AAV-2 it was demonstrated that the protein composition of crystalline virus was indistinguishable from freshly purified AAV-2, and contained the expected proportions of capsid proteins. Firstly, through measurement of OD₂₈₀ on dissolved crystals, it was demonstrated that >99% of AAV-2 in a hanging-drop had been sequestered into crystals, and that the virus crystallized was not a minor fraction. Then SDS-PAGE analysis of washed crystals, dissolved under denaturing conditions, was used to demonstrate that the composition was as expected (Fig. 4). Thus, the crystals contained the VP1 and VP2-unique regions. They are not visualized in the crystallographic electron density maps which are averaged 60-fold according to the icosahedral symmetry. Thus, VP1 and VP2 must be present at ~10% occupancies (mole fractions) that are below detectable levels, or are spatially disordered. Antigenicity, tryptic susceptibility and electron microscopy of several parvoviruses has not yet resulted in a uniform and consistent view of the location of VP1 for all parvoviruses, and it may sometimes be external to the capsid, sometimes internal, perhaps depending on species and whether the particle is empty or contains DNA (Cotmore et al., 1999; Kajigaya et al., 1991; Kronenberg et al., 2001; Rimmelzwaan et al., 1990). In all known parvoviral structures, the first residue visualized crystallographically is near the five-fold axis on the inner capsid surface. In the mammalian, but not insect parvoviruses, there is diffuse density extending from this point through a pore on the five-fold axes to the outside, suggesting that a fraction of the unseen VP1 and/or VP2 N-termini might be external (Simpson et al., 1998; Xie et al., 2002; Xie and

Chapman, 1996). The proportions of VP1, 2 and 3 mean that no more than about 6 of the 12 five-fold pores can be occupied by VP1, and no more than about 6 by VP2. There is nothing to suggest that the distribution of occupied pores would be anything but random. VP1, but perhaps not VP2, would add significant bulk to the exterior, likely affecting crystal packing contacts. It is difficult to imagine how a heterogeneous distribution of VP1 extensions over the capsid surface could be consistent with an exactly periodic crystalline lattice. This makes a circumstantial case that the N-terminus of VP1 is mostly internal in AAV-2. Although the demonstration of crystal composition has been only for AAV-2, it becomes more plausible that the other parvoviral crystals retain a full complement of capsid proteins. It is extremely difficult to envision that all of the different crystal packings would tolerate the heterogeneity of randomly placed VP1 domains to the capsid surface. VP2 has a small extension to the common VP3 core, and it is less likely to affect crystallization, no matter its location. Perhaps the differing evidence regarding internal or external location of VP1 will only be reconcilable with a dynamic equilibrium (Cotmore et al., 1999) in solution, although the crystal structures offer no hints on how the pore could be opened to allow passage of a ~200 residue polypeptide.

4.5. Implications for gene therapy

Through optimization of the propagation, it has been possible to produce efficiently larger quantities of AAV-2 than has previously been possible for either wild-type or recombinant rAAV. The methods of purification used here would not be suitable for clinical-grade preparations due to the potential toxicity of cesium chloride. However, the ready availability of large quantities of wild-type AAV-2 will allow the potential of alternative large scale purification methods to be explored without the limitation of the currently low yields of rAAV production methods. The work also demonstrates the potential benefits of glycerol or other co-solvents in manipulating concentrate solutions of AAV. Finally, the large-scale preparation methods and crystallization were required for the atomic structure determination of AAV-2 (Xie et al., 2002) that is now facilitating the development of modified rAAV vectors with altered cellular targeting and antigenicity (Huttner et al., 2003; Rabinowitz and Samulski, 2002).

Acknowledgements

We thank members of the laboratory of Ken Berns for their invitation to visit and learn the prior methods of AAV-2 propagation. Irene Davidovitch, Pam Pruet, Smita Bhatia and Connie Alford contributed to preliminary experiments. The research was supported by the American Cancer Society (F-95FSU-2 and RPG-99-356-01-GMC) and the National Institutes of Health (R01-GM066875).

References

- Agbandje, M., McKenna, R., Rossmann, M.G., Strassheim, M.L., Parsh, C.R., 1993. Structure determination of feline panleukopenia virus empty capsids. *Proteins* 16, 155–171.
- Agbandje-McKenna, M., Llamas-Saiz, A.L., Wang, F., Tattersall, P., Rossmann, M.G., 1998. Functional implications of the structure of the murine parvovirus, minute virus of mice. *Structure* 6, 1369–1381.
- Anderson, R., Macdonald, I., Corbett, T., Whiteway, A., Prentice, H.G., 2000. A method for the preparation of highly purified adeno-associated virus using affinity column chromatography, protease digestion and solvent extraction. *J. Virol. Methods* 85, 23–34.
- Auricchio, A., Hildinger, M., O'Connor, E., Gao, G.P., Wilson, J.M., 2001. Isolation of highly infectious and pure adeno-associated virus type 2 vectors with a single-step gravity-flow column. *Hum. Gene Ther.* 12, 71–76.
- Bartlett, J.S., Kleinschmidt, J., Boucher, R.C., Samulski, R.J., 1999. Targeted adeno-associated virus vector transduction of nonpermissive cells mediated by a bispecific F(ab'gamma)2 antibody. *Nat. Biotechnol.* 17, 181–186.
- Batchu, R.B., Hermonat, P.L., 1995. Disassociation of conventional DNA binding and endonuclease activities by an adeno-associated virus Rep78 mutant. *Biochem. Biophys. Res. Commun.* 210, 717–725.
- Bueler, H., 1999. Adeno-associated viral vectors for gene transfer and gene therapy. *Biol. Chem.* 380, 613–622.
- Buning, H., Ried, M.U., Perabo, L., Gerner, F.M., Huttner, N.A., Enssle, J., Hallek, M., 2003. Receptor targeting of adeno-associated virus vectors. *Gene Ther.* 10, 1142–1151.
- Cao, L., Liu, Y., During, M.J., Xiao, W., 2000. High-titer, wild-type free recombinant adeno-associated virus vector production using intron-containing helper plasmids [in process citation]. *J. Virol.* 74, 11456–11463.
- Carter, B.J., 1990. Adeno-Associated Virus Helper Functions Handbook of Parvoviruses, vol. 1. CRC Press, Boca Raton, FL, pp. 255–282.
- Chapman, M.S., Rossmann, M.G., 1995. Single-stranded DNA-protein interactions in canine parvovirus. *Structure* 3, 151–162.
- Chayen, N.E., Stewart, P.D.S., Blow, D.M., 1992. Microbatch crystallization under oil – a new technique allowing many small-volume crystallization trials. *J. Crystal Growth* 122, 176–180.
- Chiorini, J.A., Wiener, S.M., Yang, L., Smith, R.H., Safer, B., Kilcoin, N.P., Liu, Y., Urcelay, E., Kotin, R.M., 1996. The role of AAV Rep proteins in gene expression and targeted integration. *Curr. Topics Microbiol. Immunol.* 218, 25–33.
- Clark, K.R., Liu, X., McGrath, J.P., Johnson, P.R., 1999. Highly purified recombinant adeno-associated virus vectors are biologically active and free of detectable helper and wild-type viruses. *Hum. Gene Ther.* 10, 1031–1039.
- Clark, K.R., Voulgaropoulou, F., Fraley, D.M., Johnson, P.R., 1995. Cell lines for the production of recombinant adeno-associated virus. *Hum. Gene Ther.* 6, 1329–1341.
- Cotmore, S.F., D'Abramo, A., Ticknor Jr., M., Tattersall, C.M.P., 1999. Controlled conformational transitions in the MVM virion expose the VP1 N-terminus and viral genome without particle disassembly. *Virology* 254, 169–181.
- Davis, M.D., Wu, J., Owens, R.A., 2000. Mutational analysis of adeno-associated virus type 2 rep68 protein endonuclease activity on partially single-stranded substrates. *J. Virol.* 74, 2936–2942.
- de la Maza, L.M., Carter, B.J., 1980. Heavy and light particles of adeno-associated virus. *J. Virol.* 33, 1129–1137.
- Drittanti, L., Rivet, C., Manceau, P., Danos, O., Vega, M., 2000. High throughput production, screening and analysis of adeno-associated viral vectors. *Gene Ther.* 7, 924–929.
- Ducruix, A., Giegé, R. (Eds.), 1999. Crystallization of Nucleic Acids and Proteins. Oxford, Oxford.
- Ducruix, A.F., Ries-Krautt, M.M., 1990. Solubility diagram analysis and the relative effectiveness of different ions on protein crystal growth. *Methods Companion Methods Enzymol.* 1, 25–30.
- Freifelder, D., 1982. Physical Biochemistry. W.H. Freeman, New York.
- Girod, A., Ried, M., Wobus, C., Lahm, H., Leike, K., Kleinschmidt, J., Deleage, G., Hallek, M., 1999. Genetic capsid modifications allow efficient re-targeting of adeno-associated virus type 2. *Nat. Med.* 5, 1052–1056.
- Girod, A., Wobus, C.E., Zadori, Z., Ried, M., Leike, K., Tijssen, P., Kleinschmidt, J.A., Hallek, M., 2002. The VP1 capsid protein of adeno-associated virus type 2 is carrying a phospholipase A2 domain required for virus infectivity. *J. Gen. Virol.* 83, 973–978.
- Grifman, M., Trepel, M., Speece, P., Gilbert, L.B., Arap, W., Pasqualini, R., Weitzman, M.D., 2001. Incorporation of tumor-targeting peptides into recombinant adeno-associated virus capsids. *Mol. Ther.* 3, 964–975.
- Grimm, D., Kern, A., Rittner, K., Kleinschmidt, J.A., 1998. Novel tools for production and purification of recombinant adeno-associated virus vectors. *Hum. Gene Ther.* 9, 2745–2760.
- Grimm, D., Kleinschmidt, J.A., 1999. Progress in adeno-associated virus type 2 vector production: promises and prospects for clinical use. *Hum. Gene Ther.* 10, 2445–2450.
- Hampel, A., Labanauskas, M., Connors, P.G., Kirkegaard, L., RajBhandary, U.L., Sigler, P.B., Bock, R.M., 1968. Single crystals of transfer RNA from formylmethionine and phenylalanine transfer RNAs. *Science* 162, 1384–1387.
- Hermonat, P.L., Labow, M.A., Wright, R., Berns, K.I., Muzyczka, N., 1984. Genetics of adeno-associated virus: isolation and preliminary characterization of adeno-associated virus type 2 mutants. *J. Virol.* 51, 329–339.
- Hermonat, P.L., Quirk, J.G., Bishop, B.M., Han, L., 1997. The packaging capacity of adeno-associated virus (AAV) and the potential for wild-type-plus AAV gene therapy vectors. *FEBS Lett.* 407, 78–84.
- Hermonat, P.L., Santin, A.D., Batchu, R.B., Zhan, D., 1998. The adeno-associated virus Rep78 major regulatory protein binds the cellular TATA-binding protein in vitro and in vivo. *Virology* 245, 120–127.
- Hoque, M., Ishizu, K., Matsumoto, A., Han, S.I., Arisaka, F., Takayama, M., Suzuki, K., Kato, K., Kanda, T., Watanabe, H., Handa, H., 1999. Nuclear transport of the major capsid protein is essential for adeno-associated virus capsid formation. *J. Virol.* 73, 7912–7915.
- Huttner, N.A., Girod, A., Perabo, L., Edbauer, D., Kleinschmidt, J.A., Buning, H., Hallek, M., 2003. Genetic modifications of the adeno-associated virus type 2 capsid reduce the affinity and the neutralizing effects of human serum antibodies. *Gene Ther.* 10, 2139–2147.
- Im, D.-S., Muzyczka, N., 1990. The AAV origin binding protein Rep68 is an ATP-dependent site-specific endonuclease with DNA helicase activity. *Cell* 61, 447–457.
- Inoue, N., Russell, D.W., 1998. Packaging cells based on inducible gene amplification for the production of adeno-associated virus vectors. *J. Virol.* 72, 7024–7031.
- Johnson, F.B., 1984. Parvovirus proteins. In: Berns, K.I. (Ed.), *The Parvoviruses*. Plenum, New York.
- Jokoby, W.B., Pastan, I.H., 1979. *Cell Culture*, vol. 58. Academic Press, San Diego.
- Kajigaya, S., Fujii, H., Field, A., Anderson, S., Rosenfeld, S., Anderson, L.J., Shimada, T., Young, N.S., 1991. Self-assembled B19 parvovirus capsids, produced in a baculovirus expression system, are antigenically and immunogenically similar to native virions. In: *Proceedings of the National Academy of Sciences, USA*, pp. 4646–4650.
- Kaludov, N., Handelman, B., Chiorini, J.A., 2002. Scalable purification of adeno-associated virus type 2, 4 or 5 using ion-exchange chromatography. *Hum. Gene Ther.* 13, 1235–1243.
- Kogure, K., Urabe, M., Mizukami, H., Kume, A., Sato, Y., Monahan, J., Ozawa, K., 2001. Targeted integration of foreign DNA into a defined locus on chromosome 19 in K562 cells using AAV-derived components. *Int. J. Hematol.* 73, 469–475.
- Kronenberg, S., Kleinschmidt, J.A., Bottcher, B., 2001. Electron cryo-microscopy and image reconstruction of adeno-associated virus type 2 empty capsids. *EMBO Reports* 2 (11), 997–1002.

- Laughlin, C.A., Tratschin, J.D., Coon, H., Carter, B.J., 1983. Cloning of infectious adeno-associated virus genomes in bacterial plasmids. *Gene* 23, 65–73.
- Li, J., Samulski, R.J., Xiao, X., 1997. Role for highly regulated rep gene expression in adeno-associated virus vector production. *J. Virol.* 71, 5236–5243.
- Linden, R.M., Ward, P., Giraud, C., Winocour, E., Berns, K.I., 1996. Site-specific integration by adeno-associated virus. In: *Proceedings of the National Academy of Sciences, USA*, pp. 11288–11294.
- Luft, J.R., Titta, G.T., 1996. Chaperone salts, polyethylene glycol and rates of equilibration in vapor-diffusion crystallization. *Acta Crystallogr. D51*, 780–785.
- Matsushita, T., Elliger, S., Elliger, C., Podsakoff, G., Villarreal, L., Kurtzman, G.J., Iwaki, Y., Colosi, P., 1998. Adeno-associated virus vectors can be efficiently produced without helper virus. *Gene Ther.* 5, 938–945.
- McPherson, A., 1990. Current approaches to macromolecular crystallization. *Eur. J. Biochem.* 189, 1–23.
- McPherson, A., 1998. *Crystallization of biological macromolecules*. Cold Spring Harbor Laboratory Press, Cold Spring Harbor, NY.
- Mizukami, H., Young, N., Brown, K., 1996. Adeno-associated virus type 2 binds to a 150-kilodalton cell membrane glyco protein. *Virology* 217, 124–130.
- Moskalenko, M., Chen, L., van Roey, M., Donahue, B.A., Snyder, R.O., McArthur, J.G., Patel, S.D., 2000. Epitope mapping of human anti-adeno-associated virus type 2 neutralizing antibodies: implications for gene therapy and virus structure. *J. Virol.* 74, 1761–1766.
- Ogasawara, Y., Urabe, M., Kogure, K., Kume, A., Colosi, P., Kurtzman, G.J., Ozawa, K., 1999. Efficient production of adeno-associated virus vectors using split-type helper plasmids. *Jpn. J. Cancer Res.* 90, 476–483.
- O’Riordan, C.R., Lachapelle, A.L., Vincent, K.A., Wadsworth, S.C., 2000. Scaleable chromatographic purification process for recombinant adeno-associated virus (rAAV). *J. Gene Med.* 2, 444–454.
- Potter, M., Chesnut, K., Muzyczka, N., Flotte, T., Zolotukhin, S., 2002. Streamlined large-scale production of recombinant adeno-associated virus (rAAV) vectors. *Methods Enzymol.* 346, 413–430.
- Qiu, J., Handa, A., Kirby, M., Brown, K.E., 2000. The interaction of heparin sulfate and adeno-associated virus 2. *Virology* 269, 137–147.
- Rabinowitz, J., Samulski, R., 2002. The adeno-associated virus crystal: impact inversely proportional to size. *Mol. Ther.* 6, 443.
- Ried, M.U., Girod, A., Leike, K., Buning, H., Hallek, M., 2002. Adeno-associated virus capsids displaying immunoglobulin-binding domains permit antibody-mediated vector retargeting to specific cell surface receptors. *J. Virol.* 76, 4559–4566.
- Rimmelzwaan, G.F., Carlson, J., UytdeHaag, F.G.C.M., Osterhaus, A.D.M.E., 1990. A synthetic peptide derived from the amino acid sequence of canine parvovirus structural proteins which defines a B cell epitope and elicits antiviral antibody in BALB c mice. *J. Gen. Virol.* 71, 2741–2745.
- Rodgers, D.W., 1994. Cryocrystallography. *Structure* 2, 1135–1140.
- Rose, J.A., Maizel Jr., J.V., Inman, J.K., Shatkin, A.J., 1971. Structural protein of adenovirus-associated viruses. *J. Virol.* 8, 766–770.
- Seisenberger, G., Ried, M.U., Endress, T., Buning, H., Hallek, M., Brauchle, C., 2001. Real-time single-molecule imaging of the infection pathway of an adeno-associated virus. *Science* 294, 1929–1932.
- Simpson, A.A., Chipman, P.R., Baker, T.S., Tijssen, P., Rossmann, M.G., 1998. The structure of an insect parvovirus (*Galleria mellonella* densovirus) at 3.7 Å resolution. *Structure* 6, 1355–1367.
- Simpson, A.A., Hebert, B., Sullivan, G.M., Parrish, C.R., Zadori, Z., Tijssen, P., Rossmann, M.G., 2002. The structure of porcine parvovirus: comparison with related viruses. *J. Mol. Biol.* 315, 1189–1198.
- Sommer, J.J., Smith, P.H., Parthasarathy, S., Isaacs, J., Vijay, S., Kieran, J., Powell, S.K., McClelland, A., Wright, J.F., 2003. Quantification of adeno-associated virus particles and empty capsids by optical density measurement. *Mol. Ther.* 7, 122–128.
- Summerford, C., Samulski, R.J., 1998. Membrane-associated heparan sulfate proteoglycan is a receptor for adeno-associated virus type 2 virions. *J. Virol.* 72, 1438–1445.
- Summerford, C., Samulski, R.J., 1999. Viral receptors and vector purification: new approaches for generating clinical-grade reagents. *Nat. Med.* 5, 587–588.
- Tamayose, K., Hirai, Y., Shimada, T., 1996. A new strategy for large scale preparation of high-titer recombinant adeno-associated virus vectors by packaging cell lines and sulfonated cellulose column chromatography. *Hum. Gene Ther.* 7, 507–513.
- Tsao, J., Chapman, M.S., Agbandje, M., Keller, W., Smith, K., Wu, H., Luo, M., Smith, T.J., Rossmann, M.G., Compans, R.W., Parrish, C., 1991. The three-dimensional structure of canine parvovirus and its functional implications. *Science* 251, 1456–1464.
- Urabe, M., Ding, C., Kotin, R.M., 2002. Insect cells as a factory to produce adeno-associated virus type 2 vectors. *Hum. Gene Ther.* 13, 1935–1943.
- Urabe, M., Shimazaki, K., Saga, Y., Okada, T., Kume, A., Tobita, K., Ozawa, K., 2000. Self-amplification system for recombinant adeno-associated virus production [in process citation]. *Biochem. Biophys. Res. Commun.* 276, 559–563.
- Vincent, K.A., Piraino, S.T., Wadsworth, S.C., 1997. Analysis of recombinant adeno-associated virus packaging and requirements for rep and cap gene products. *J. Virol.* 71, 1897–1905.
- Walsh, L., Tuma, R., Thoma, G.J., Bamford, D.H., 1994. Purification of viruses and macromolecular assemblies for structural investigations using a novel ion exchange method. *Virology* 201, 1–7.
- Weger, S.W.A., Grimm, D., Kleinschmidt, J.A., 1997. Control of adeno-associated virus type 2 cap gene expression: relative influence of helper virus, terminal repeats, and rep proteins. *J. Virol.* 71, 8437–8447.
- Wendtner, C.M., Kofler, D.M., Theiss, H.D., Kurzeder, C., Buhmann, R., Schweighofer, C., Perabo, L., Danhauser-Riedl, S., Baumert, J., Hiddemann, W., Hallek, M., Buning, H., 2002. Efficient gene transfer of CD40 ligand into primary B-CLL cells using recombinant adeno-associated virus (rAAV) vectors. *Blood* 100, 1655–1661.
- Winocour, E., Puzis, L., Etkin, S., Koch, T., Danovitch, B., Mendelson, E., Shaulian, E., Karby, S., Lavi, S., 1992. Modulation of the cellular phenotype by integrated adeno-associated virus. *Virology* 190, 316–329.
- Wistuba, A., Weger, S., Kern, A., Kleinschmidt, J.A., 1995. Intermediate of adeno-associated virus type 2 assembly: identification of soluble complexes containing rep and cap proteins. *J. Virol.* 69, 5311–5319.
- Wobus, C.E., Hugle-Dorr, B., Girod, A., Petersen, G., Hallek, M., Kleinschmidt, J.A., 2000. Monoclonal antibodies against the adeno-associated virus type 2 (AAV-2) capsid: epitope mapping and identification of capsid domains involved in AAV-2-cell interaction and neutralization of AAV-2 infection. *J. Virol.* 74, 9281–9293.
- Wu, P., Xiao, W., Conlon, T., Hughes, J., Agbandje-McKenna, M., Ferkol, T., Flotte, T., Muzyczka, N., 2000. Mutational analysis of the adeno-associated virus type 2 (AAV2) capsid gene and construction of AAV2 vectors with altered tropism. *J. Virol.* 74, 8635–8647.
- Xie, Q., Bu, W., Bhatia, S., Hare, J., Somasundaram, T., Azzi, A., Chapman, M.S., 2002. The atomic structure of adeno-associated virus (AAV-2), a vector for human gene therapy. *Proc. Natl. Acad. Sci. U.S.A.* 99, 10405–10410.
- Xie, Q., Chapman, M.S., 1996. Canine parvovirus capsid structure, analyzed at 2.9 Å resolution. *J. Mol. Biol.* 264, 497–520.
- Young Jr., S.M., McCarty, D.M., Degtyareva, N., Samulski, R.J., 2000. Roles of adeno-associated virus Rep protein and human chromosome 19 in site-specific recombination. *J. Virol.* 74, 3953–3966.
- Zolotukhin, S., Byrne, B., Mason, E., Zolotukhin, I., Potter, M., Chesnut, K., Summerford, C., Samulski, R., Muzyczka, N., 1999. Recombinant adeno-associated virus purification using novel methods improves infectious titer and yield. *Gene Ther.* 6, 973–985.